Low-Z Impurity Transport Analysis by Transient Gas Puff Experiments

Comparisons With Neoclassical and Turbulent Predictions

By Stuart Henderson [1]

with

L. Garzotti [2], H. Meyer [2], M. O'Mullane [1], A. Patel [2], H. Summers [1], M. Valovič [2] and the MAST team

[1] Departments of Physics SUPA, University of Strathclyde, Glasgow, G4 ONG, UK

[2] EURATOM/CCFE Fusion Association, Culham Science Centre, Abingdon, Oxfordshire, OX14 3DB

Work supported by the RCUK Energy Programme and EURATOM

CCFE
CULHAM CENTRE FOR FUSION ENERGY

Outline

- **Motivation for studying impurity transport**
- **Experimental method of extracting transport coefficients**
- **Changing dynamics during a neoclassical and anomalous regime**
- **Ongoing work**
- **Conclusions**

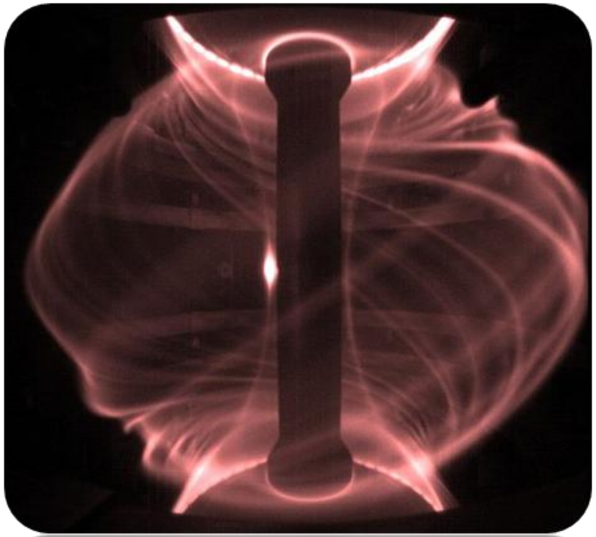

Motivation

Peaked low-Z impurity profile dynamics have important implications for fusion devices

- **Fuel dilution**
- **Loss of core temperature due to impurity line emission and Bremsstrahlung emission**

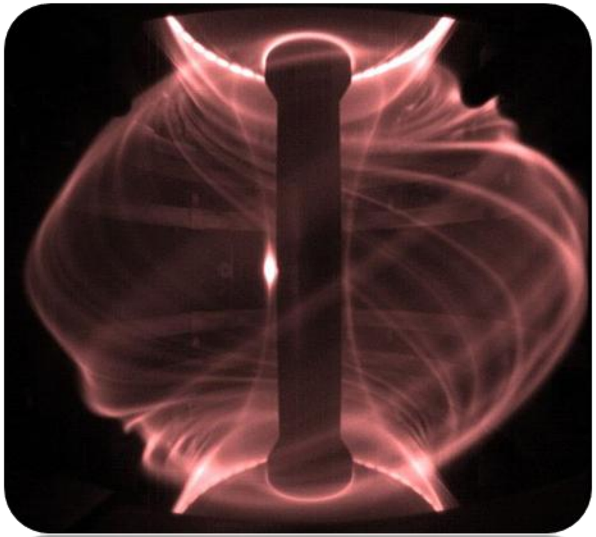

Motivation

Peaked low-Z impurity profile dynamics have important implications for fusion devices

- **Fuel dilution**
- **Loss of core temperature due to impurity line emission and Bremsstrahlung emission**

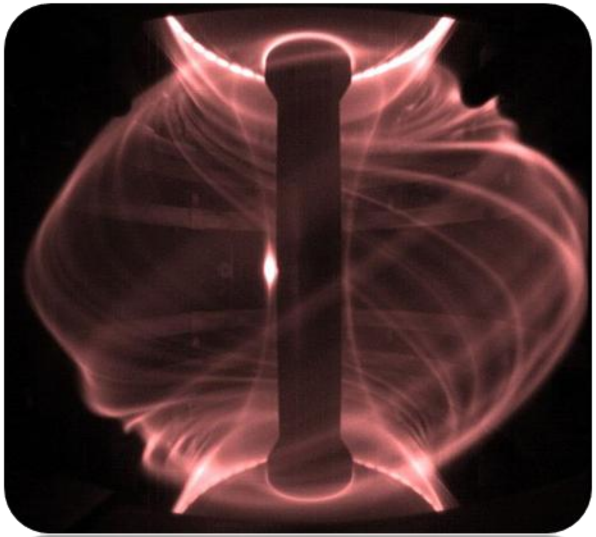

Experimental impurity transport measurements on spherical tokamaks are limited [1,2,3]

- **First transport analysis of helium and carbon**

[1] D. Stutman, M. Finkenthal, R. Bell, *et al*, Phys. Plasmas, **10**, 4387 (2003)
[2] L. Delgado-Aparicio, D. Stutman, K. Tritz, *et al*, Nucl. Fusion, **49**, 085028 (2009)
[3] I. Lehane, G. Turri, R. Akers, *et al*, 30th EPS Conference, **27A**, 3 (2003)

Motivation

Peaked low-Z impurity profile dynamics have important implications for fusion devices

- Fuel dilution
- Loss of core temperature due to impurity line emission and Bremsstrahlung emission

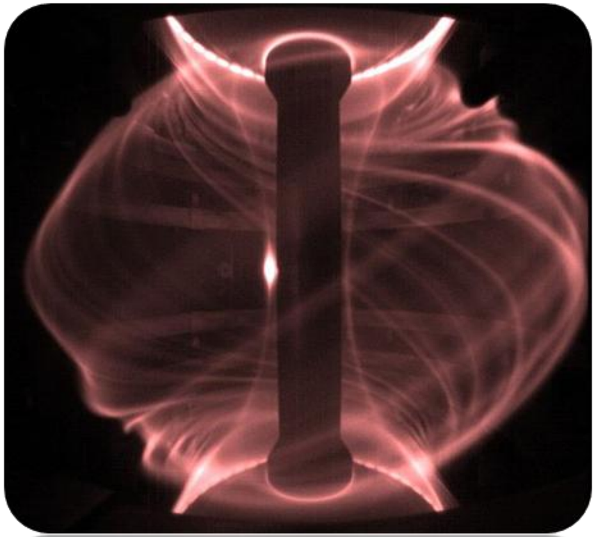

Experimental impurity transport measurements on spherical tokamaks are limited [1,2,3]

- First transport analysis of helium and carbon

Some aspects of fluid model theories describing anomalous impurity transport have yet to be experimentally tested [4]

[4] C. Angioni and A. Peeters, Phys. Rev. Lett., **96**, 1 (2006)

Experimental Method

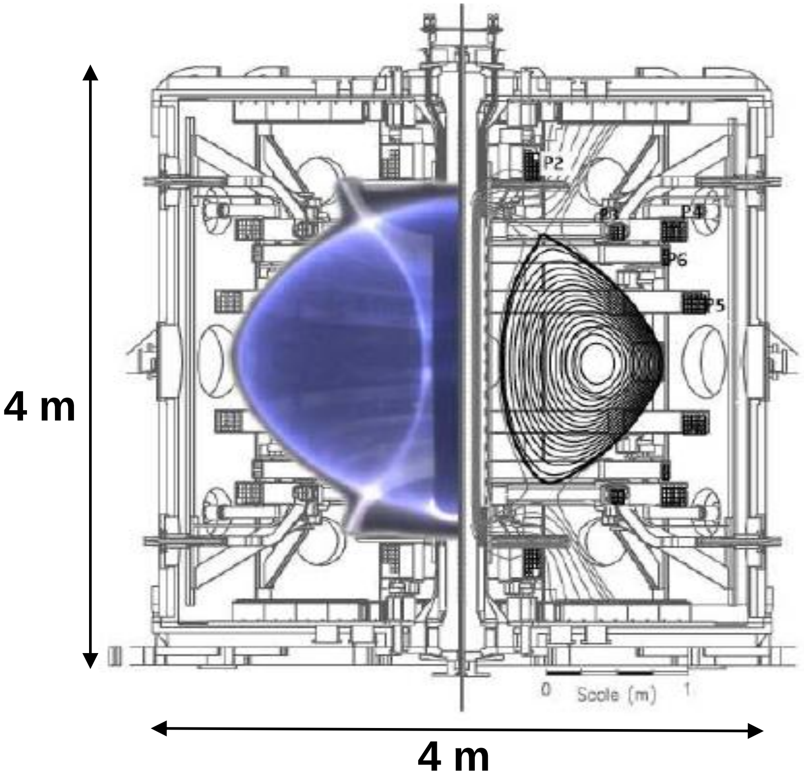

- **Perturbative Gas Puff Experiments on MAST**
  - **50 ms methane and helium injections**
  - **Plasma current scan [0.6 MA, 0.9 MA]**
  - **Confinement scan [L- & H-mode]**

I_p = [0.6,0.9] MA
B_ϕ = 0.5 T
P_{NBI} = [1.8,3.5] MW

Experimental Method

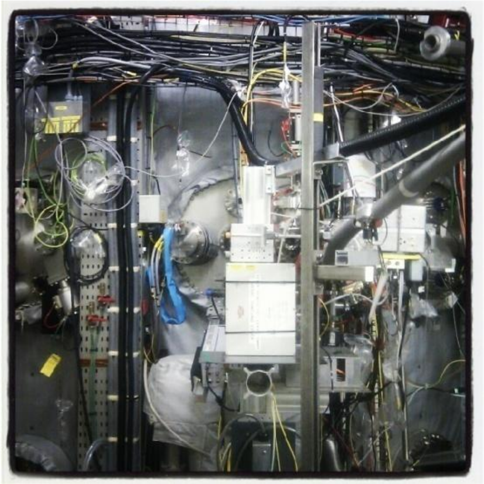

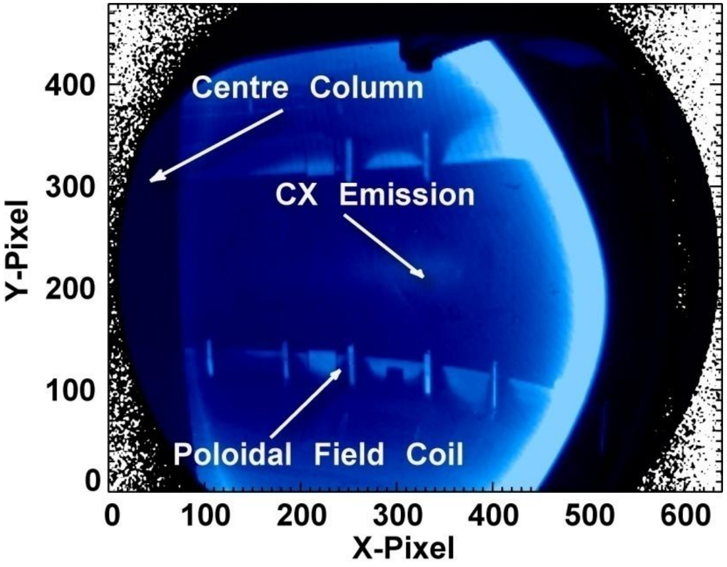

- Perturbative Gas Puff Experiments on MAST
  - 50 ms methane and helium injections
  - Plasma current scan [0.6 MA, 0.9 MA]
  - Confinement scan [L- & H-mode]

- **RGB 2D Camera [5]**
  - **Simultaneously views both CXR enhanced C^{5+} [λ=529.3 nm] and He^{+} [λ=468.8 nm] spectral lines**
  - **Plasma cross-section in VGA resolution**

[5] A. Patel *et al*, Paper Submitted, (2012)

Experimental Method

Neutral Beam Emission

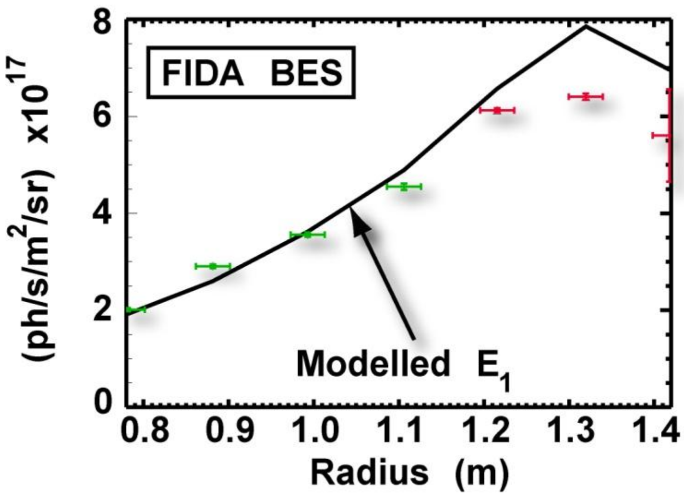

Typical Impurity Densities

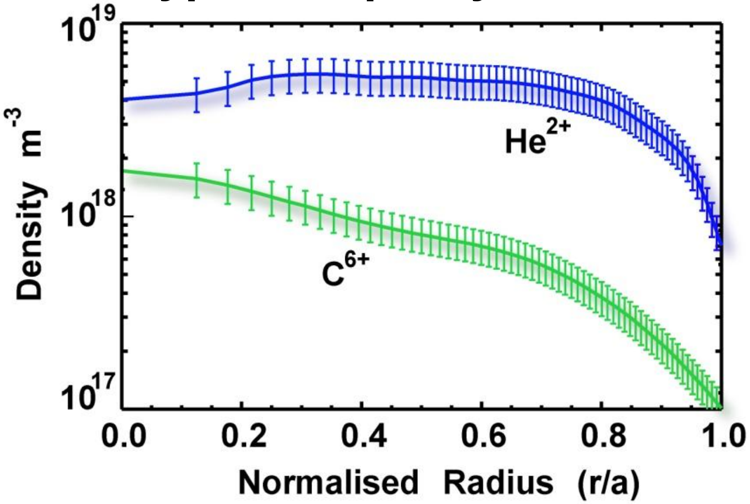

- Perturbative Gas Puff Experiments on MAST
  - 50 ms methane and helium injections
  - Plasma current scan [0.6 MA, 0.9 MA]
  - Confinement scan [L- & H-mode]
- RGB 2D Camera [5]
  - Simultaneously views both CXR enhanced C^{5+} [λ=529.3 nm] and He^{+} [λ=468.8 nm] spectral lines
  - Plasma cross-section in VGA resolution
- **Modelled Impurity Density**
  - **Beam neutrals modelled [6]**
  - **ADAS[7] effective CX emission**

[6] M. Schneider *et al*, Nucl. Fusion, **51**, 063019 (2011)
[7] H. Summers, ADAS User Manual, University of Strathclyde, **V2.7**, 2004

Transport Coefficients

- The impurity transport code, SANCO, is used to solve the coupled continuity equation

$$\frac{\partial n_z}{\partial t} = -\frac{1}{r}\frac{\partial}{\partial r}\left(r\Gamma_z\right) + \sigma_z; \quad \forall z \in [1, Z]$$ *1) Continuity Equation*

$$\Gamma_z = \Gamma_{Turb} + \Gamma_{neo} = -D_z \frac{\partial n_z}{\partial r} + v_z n_z$$ *2) Empirical Ansatz*

Transport Coefficients

• The impurity transport code, SANCO, is used to solve the coupled continuity equation

$$\frac{\partial n_z}{\partial t} = -\frac{1}{r}\frac{\partial}{\partial r}\left(r\Gamma_z\right) + \sigma_z; \quad \forall z \in [1, Z]$$

1) Continuity Equation

$$\Gamma_z = \Gamma_{Turb} + \Gamma_{neo} = -D_z \frac{\partial n_z}{\partial r} + v_z n_z$$

2) Empirical Ansatz

• Electron ionization, excitation and recombination processes which connect neighbouring charge states are modelled using ADAS

Transport Coefficients

- The impurity transport code, SANCO, is used to solve the coupled continuity equation

$$\frac{\partial n_z}{\partial t} = -\frac{1}{r}\frac{\partial}{\partial r}(r\Gamma_z) + \sigma_z; \quad \forall z \in [1, Z]$$ *1) Continuity Equation*

$$\Gamma_z = \Gamma_{Turb} + \Gamma_{neo} = -D_z \frac{\partial n_z}{\partial r} + v_z n_z$$ *2) Empirical Ansatz*

- Electron ionization, excitation and recombination processes which connect neighbouring charge states are modelled using ADAS

- Diffusivity (D) and convective velocity (v) coefficients are adjusted to minimize χ^2 between SANCO and experimental C^{6+} and He^{2+} densities

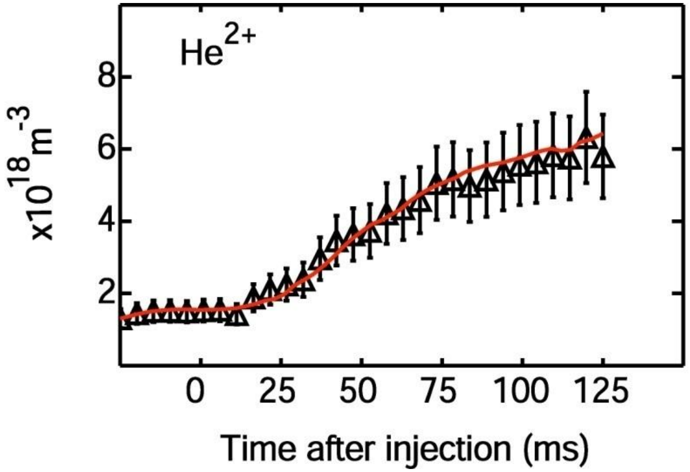

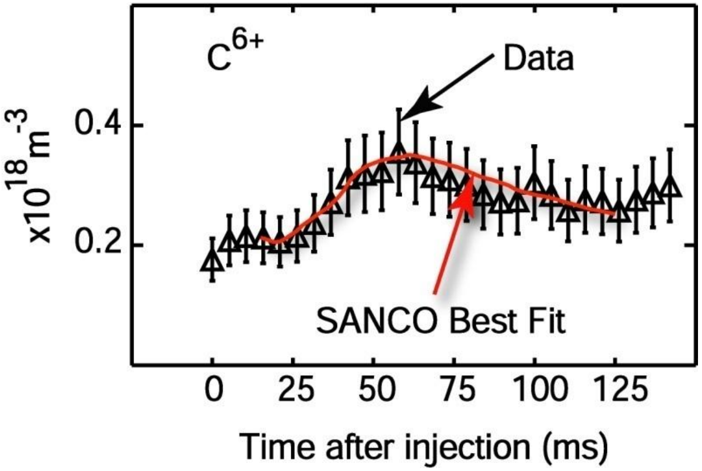

Neoclassical Effects

- **Changing dynamics during L- and H-mode**

Neoclassical Effects

- **Changing dynamics during L- and H-mode**
  - Accumulation of He^{2+} in L-mode

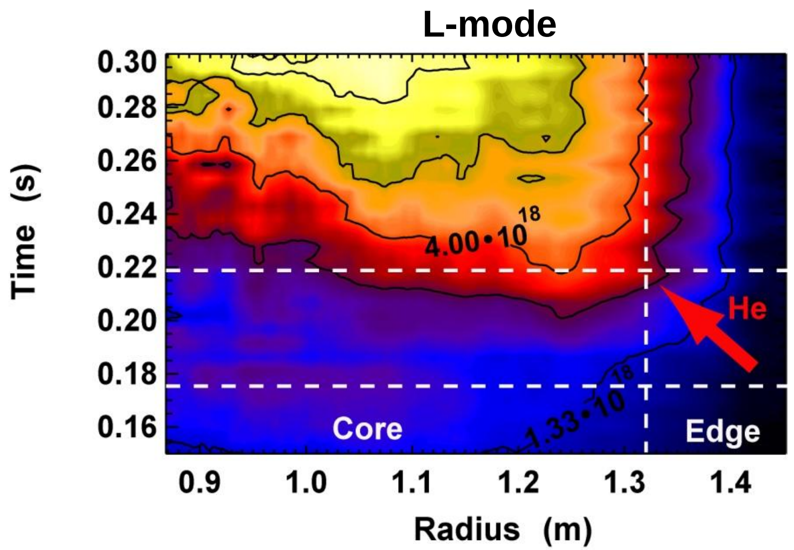

Neoclassical Effects

- **Changing dynamics during L- and H-mode**
  - Accumulation of He^{2+} in L-mode
  - Screening of He^{2+} in H-mode

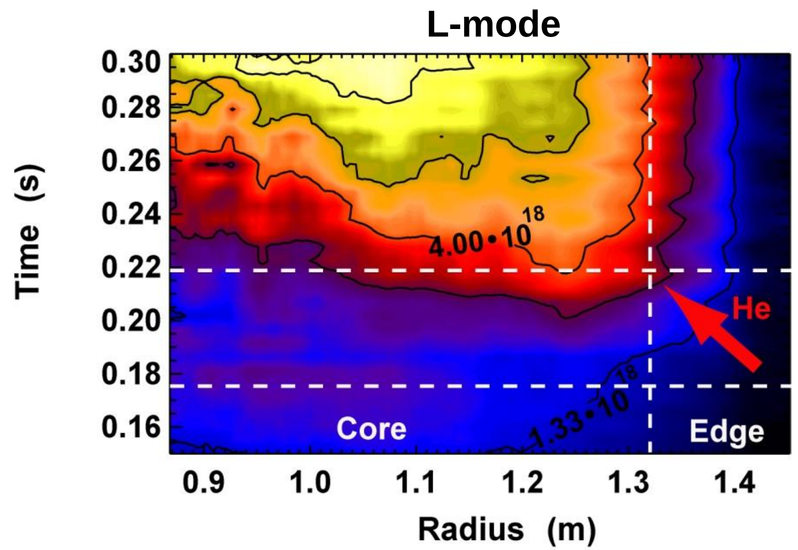

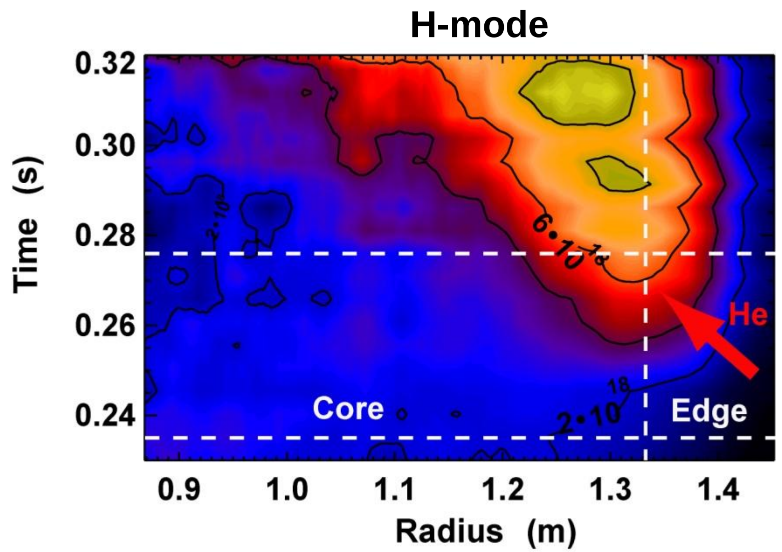

Neoclassical Effects

- **Changing dynamics during L- and H-mode**
  - ➢ Accumulation of He^{2+} in L-mode
  - ➢ Screening of He^{2+} in H-mode
- **Switch in convection direction at r/a~0.5**

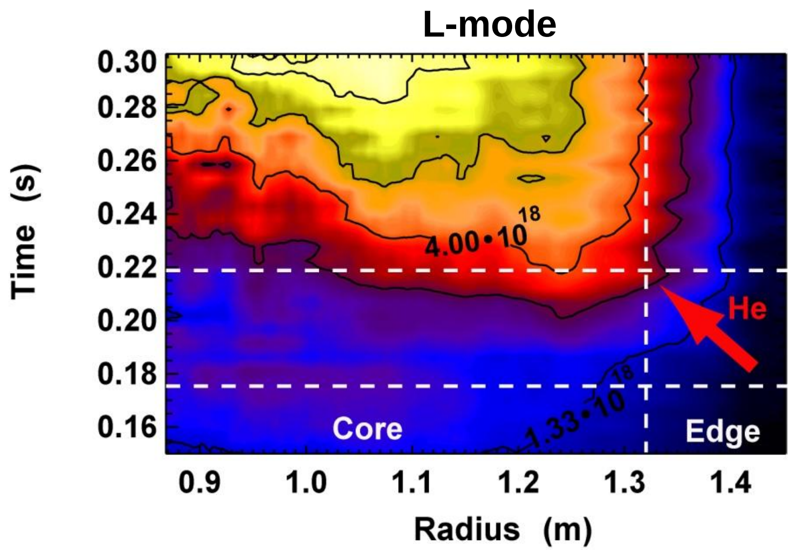

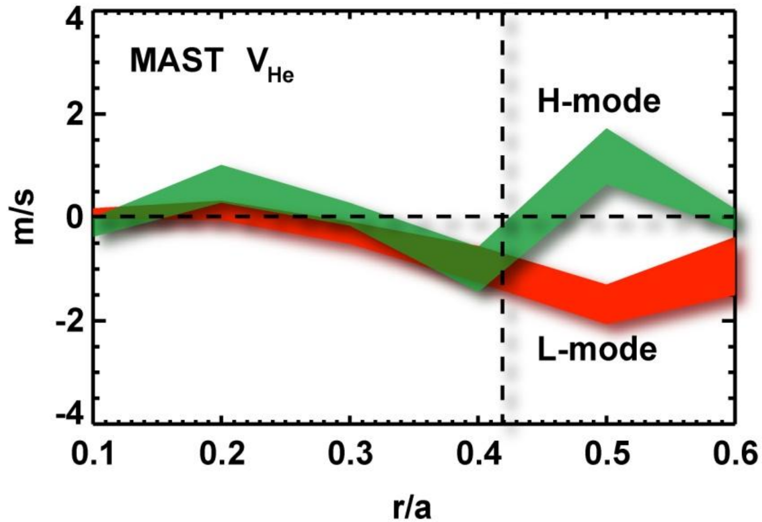

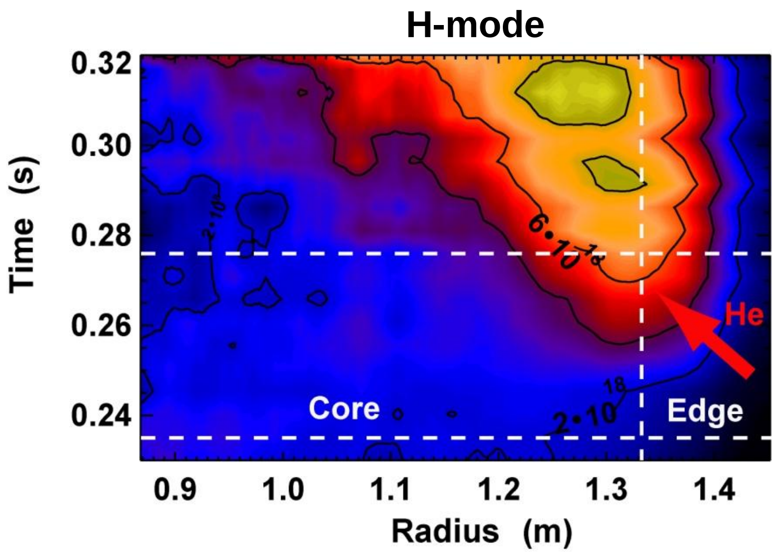

Neoclassical Effects

- **Changing dynamics during L- and H-mode**
  - Accumulation of He^{2+} in L-mode
  - Screening of He^{2+} in H-mode

- **Switch in convection direction at r/a~0.5**

- **Neoclassical theory Vs. Experiment**

$$D^{NC} \propto \frac{q^2 m_i}{B^2 \sqrt{T_i}} n_i$$

$$V^{NC} = D^{NC}\left(Z \frac{\nabla N_i}{N_i} + \alpha \frac{\nabla T_i}{T_i} \right)$$

Neoclassical Effects

- **Changing dynamics during L- and H-mode**
  - Accumulation of He^{2+} in L-mode
  - Screening of He^{2+} in H-mode

$$D^{NC} \propto \frac{q^2 m_i}{B^2 \sqrt{T_i}} n_i$$

- **Switch in convection direction at r/a~0.5**

$$V^{NC} = D^{NC}\left(Z\frac{\nabla N_i}{N_i} + \alpha \frac{\nabla T_i}{T_i} \right)$$

- **Neoclassical theory Vs. Experiment**
  - L-mode anomalous for r/a > 0.4

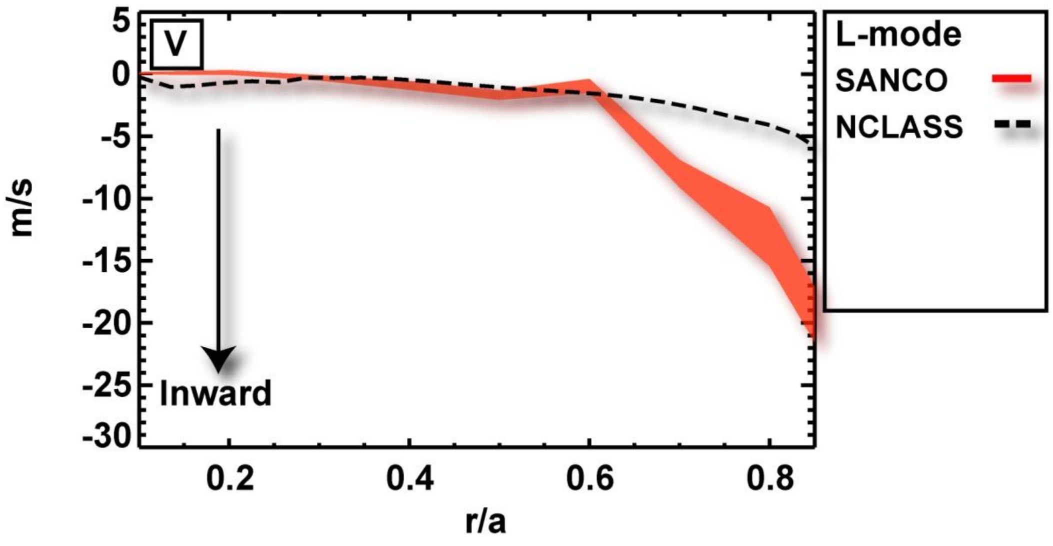

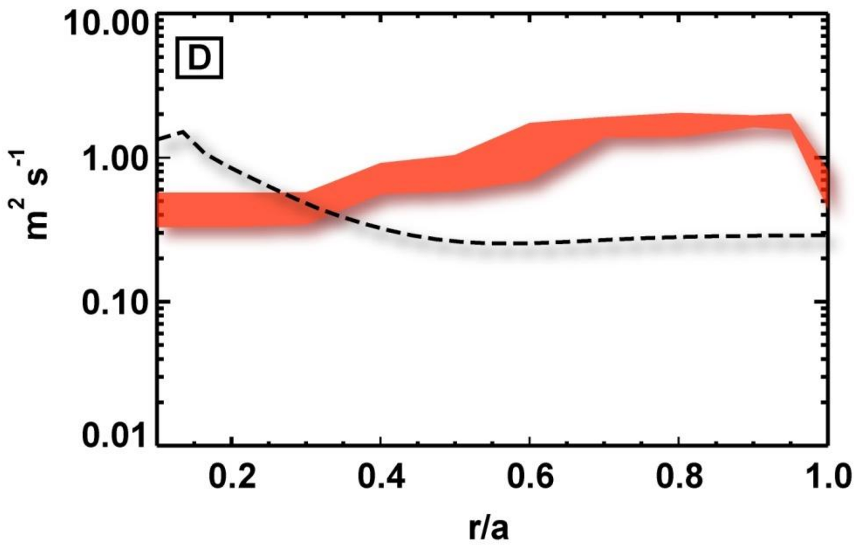

Neoclassical Effects

- **Changing dynamics during L- and H-mode**
  - Accumulation of He^{2+} in L-mode
  - Screening of He^{2+} in H-mode
- **Switch in convection direction at r/a~0.5**
- **Neoclassical theory Vs. Experiment**
  - L-mode anomalous for r/a > 0.4
  - H-mode neoclassical for r/a < 0.8

$$D^{NC} \propto \frac{q^2 m_i}{B^2 \sqrt{T_i}} n_i$$

$$V^{NC} = D^{NC}\left(Z \frac{\nabla N_i}{N_i} + \alpha \frac{\nabla T_i}{T_i} \right)$$

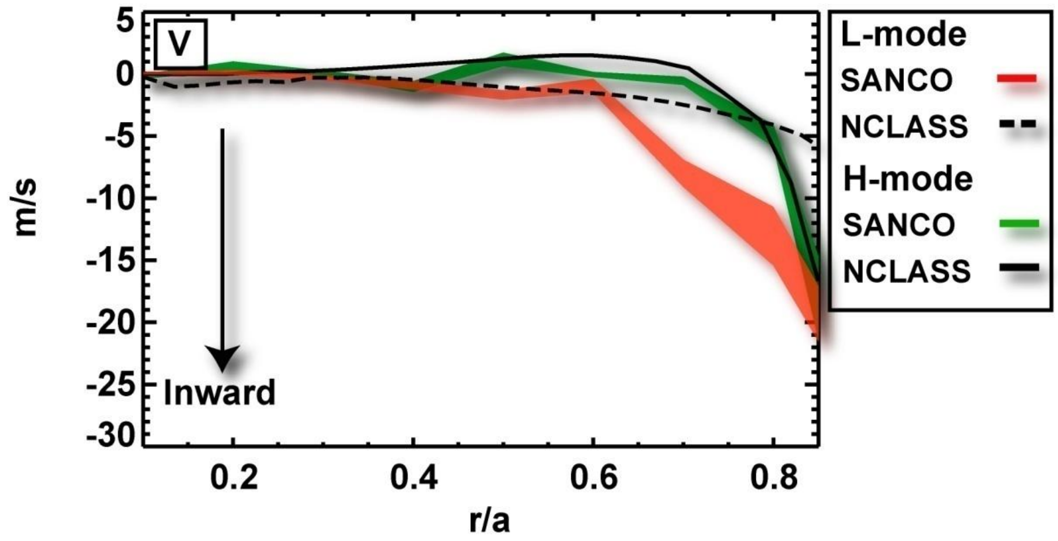

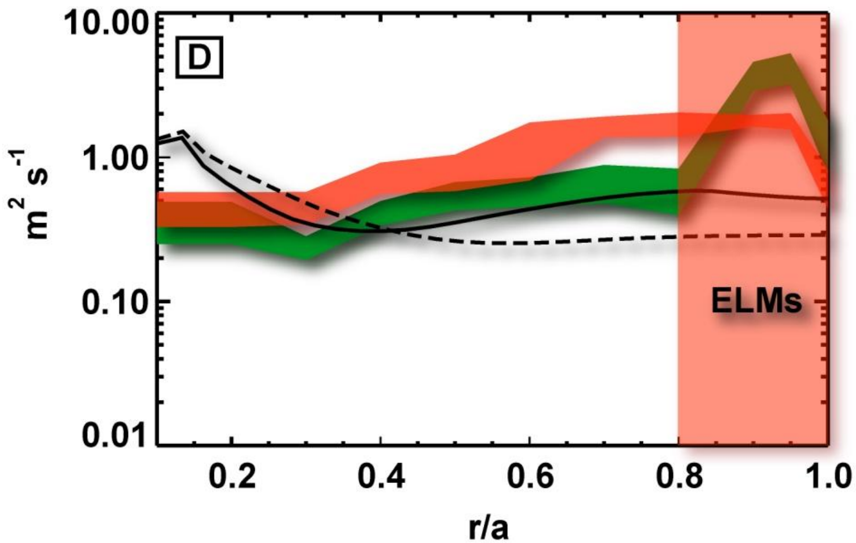

H-Mode Neoclassical Screening

Conditions For Outward Convection

$$V^{NC} = D^{NC}\left(Z \frac{\nabla N_i}{N_i} + \alpha \frac{\nabla T_i}{T_i} \right)$$

As α is typically negative,

- Weak or positive ion density gradient
- Strong ion temperature gradient

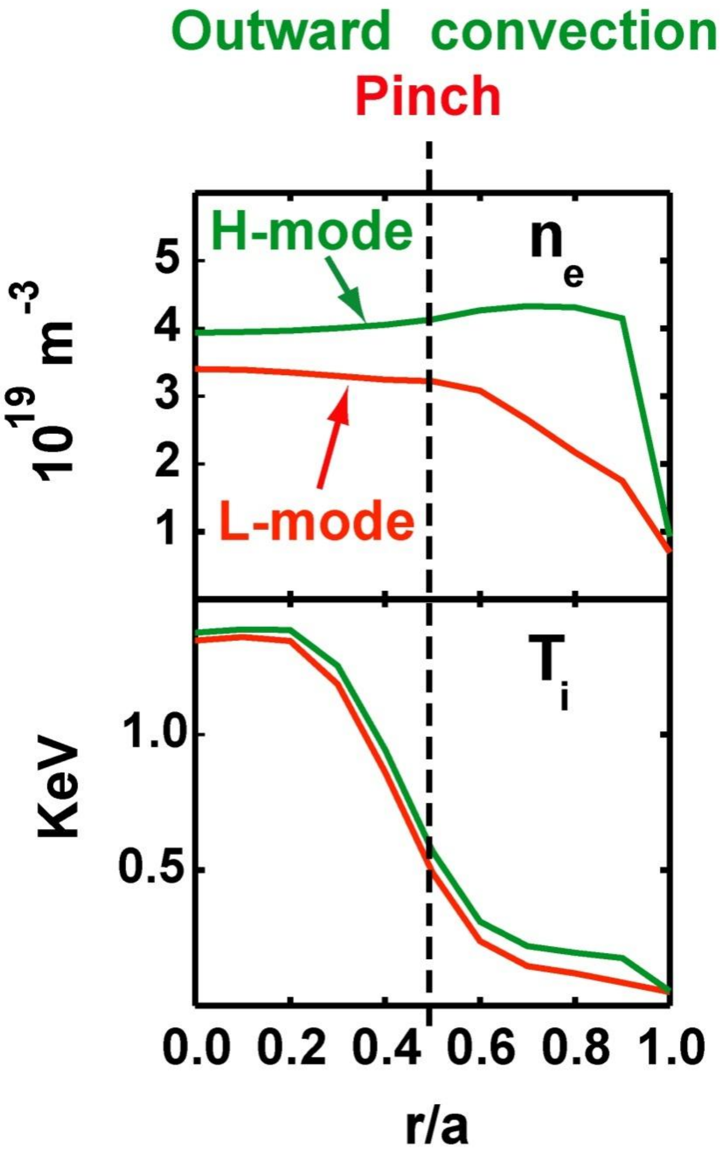

Previous NSTX Results

- **Neon gas puff experiment during an H-mode I_p-scan at constant q**
  - – L. Delgado-Aparicio, D. Stutman, K. Tritz, *et al*, Nucl. Fusion, **49**, 085028 (2009)

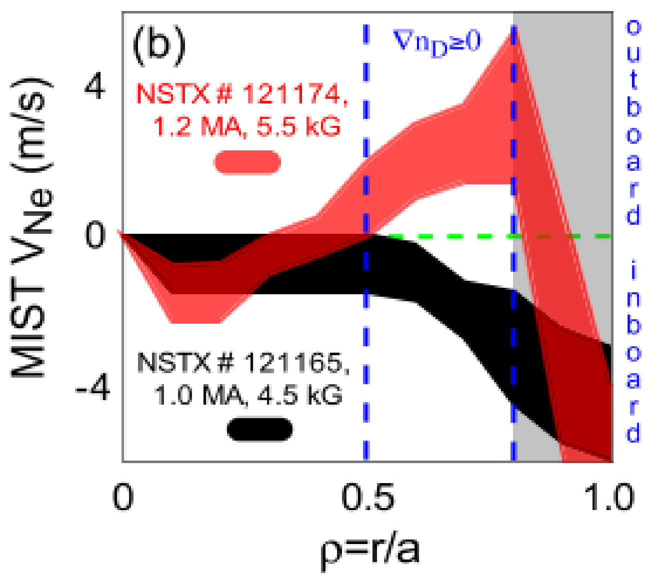

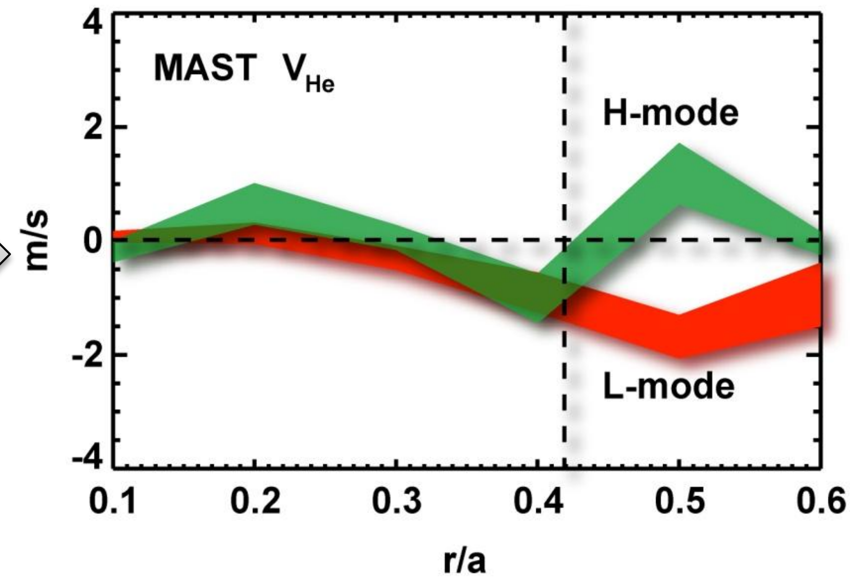

- **Outward convection in H-mode observed on both NSTX and MAST**

- **Changing dynamics during high and low I_p**

L-mode Anomalous Transport

- **Changing dynamics during high and low I_p**
  - Strong accumulation of C^{6+} in Low I_p

Low Current (I_p=0.6 MA)

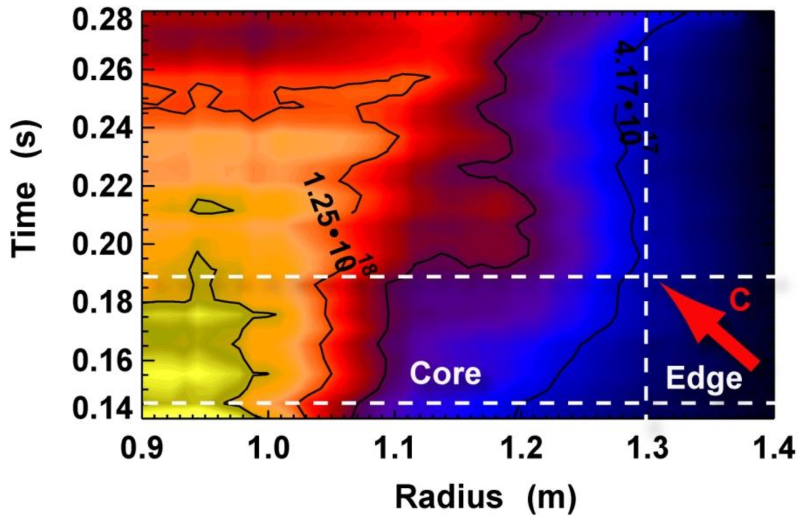

L-mode Anomalous Transport

- **Changing dynamics during high and low I_p**
  - Strong accumulation of C^{6+} in Low I_p
  - Weak accumulation of C^{6+} in High I_p

Low Current (I_p=0.6 MA)

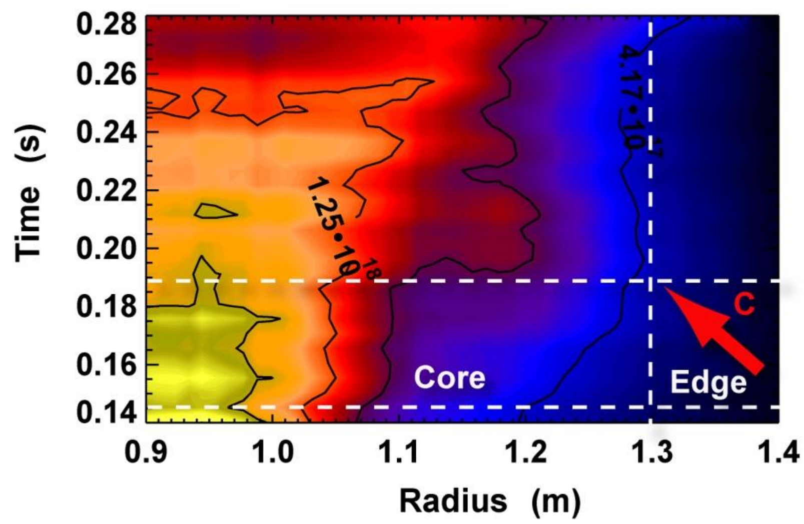

High Current (I_p=0.9 MA)

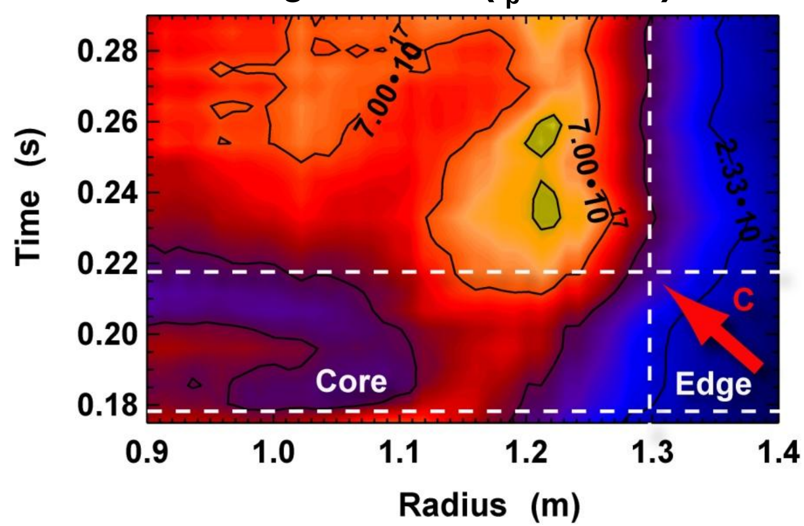

L-mode Anomalous Transport

- **Changing dynamics during high and low I_p**
  - Strong accumulation of C^{6+} in Low I_p
  - Weak accumulation of C^{6+} in High I_p

- **Trend in convection direction for r/a > 0.5**

Low Current (I_p=0.6 MA)

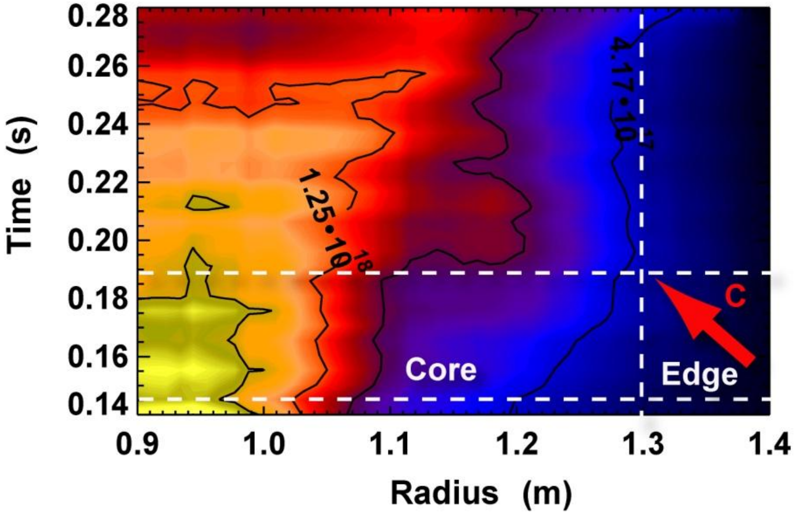

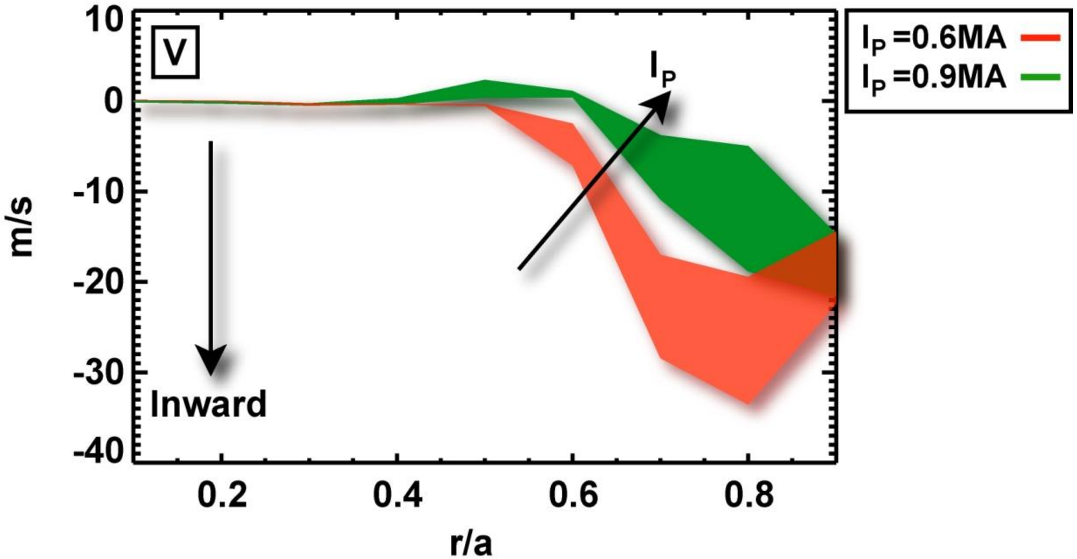

High Current (I_p=0.9 MA)

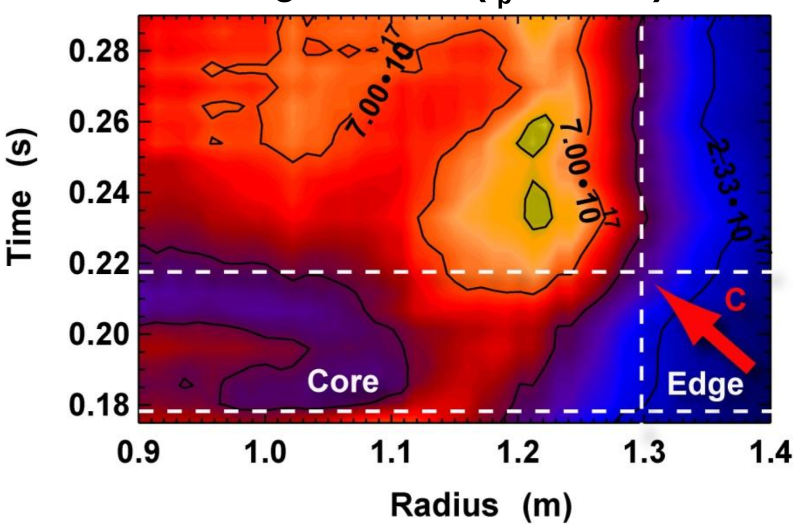

L-mode Anomalous Transport

- **Changing dynamics during high and low I_p**
  - Strong accumulation of C^{6+} in Low I_p
  - Weak accumulation of C^{6+} in High I_p
- **Trend in convection direction for r/a > 0.5**
- **Fluid Model – 3 Radial Convection Terms**

❖ **Thermodiffusion**
~ (1/Z)(R/L_{TZ})

❖ **Curvature Pinch**
~ ∇q/q

❖ **Parallel Compression**
~ (Z/Aq^2)

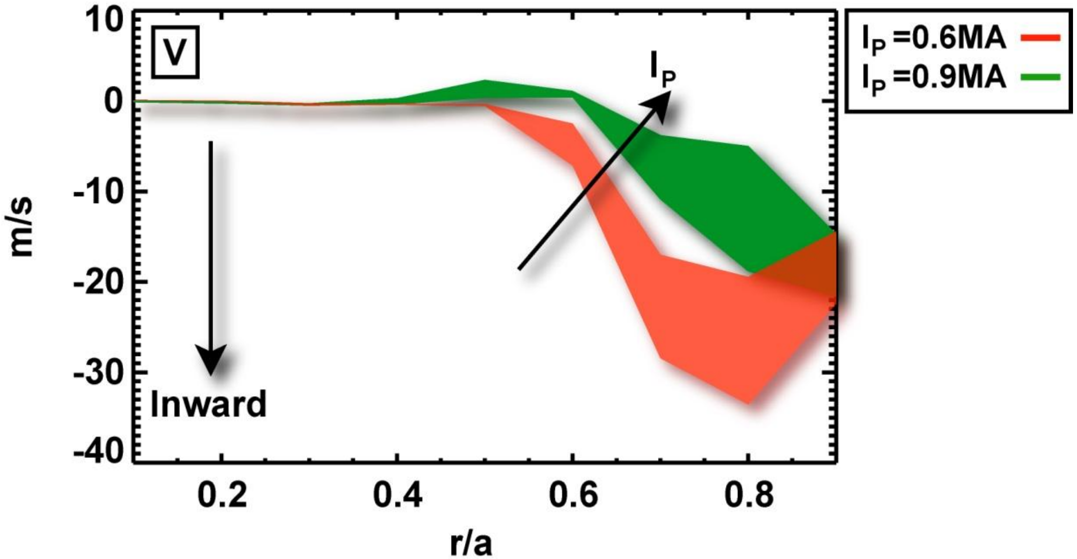

L-mode Anomalous Transport

- **Changing dynamics during high and low I_p**
  - Strong accumulation of C^{6+} in Low I_p
  - Weak accumulation of C^{6+} in High I_p
- **Trend in convection direction for r/a > 0.5**
- **Fluid Model – 3 Radial Convection Terms**
  - Sign dependent on direction of background turbulence propagation

❖ **Thermodiffusion** – ***Inwards***
~ (1/Z)(R/L$_{TZ}$)

❖ **Curvature Pinch** – ***Inwards***
~ ∇q/q

❖ **Parallel Compression** – ***Outwards***
~ (Z/Aq^2)

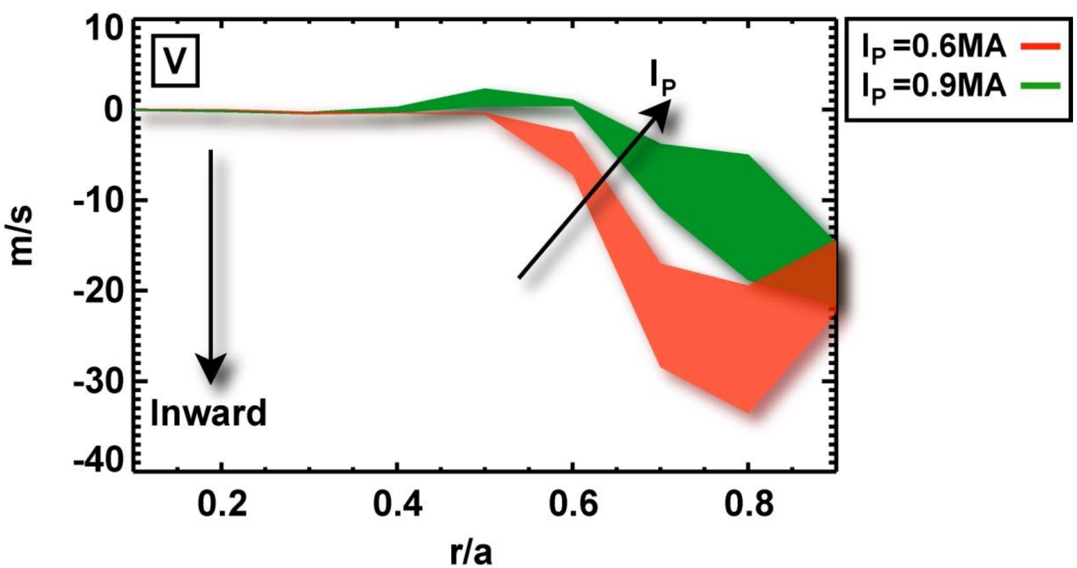

In the outer regions of the plasma, the background turbulence is rotating in the electron diamagnetic direction

L-mode Anomalous Transport

- **Changing dynamics during high and low I_p**
  - Strong accumulation of C^{6+} in Low I_p
  - Weak accumulation of C^{6+} in High I_p
- **Trend in convection direction for r/a > 0.5**
- **Fluid Model – 3 Radial Convection Terms**
  - Sign dependent on direction of background turbulence propagation
  - Changing q-profile suggests trend

❖ **Thermodiffusion** – ***Inwards***
~ $(1/Z)(R/L_{TZ})$

❖ **Curvature Pinch** – ***Inwards***
~ $\nabla q/q$

❖ **Parallel Compression** – ***Outwards***
~ (Z/Aq^2)

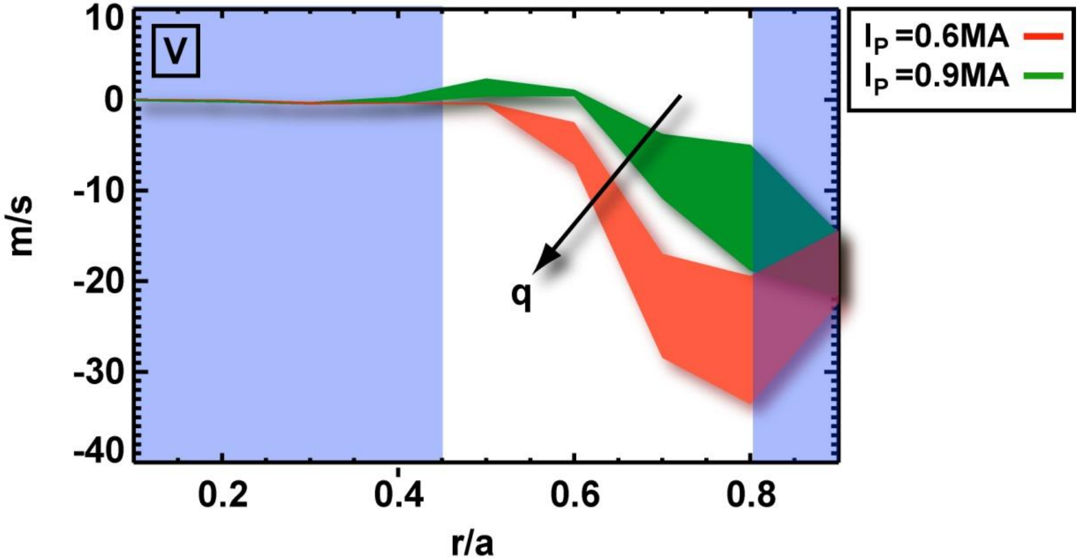

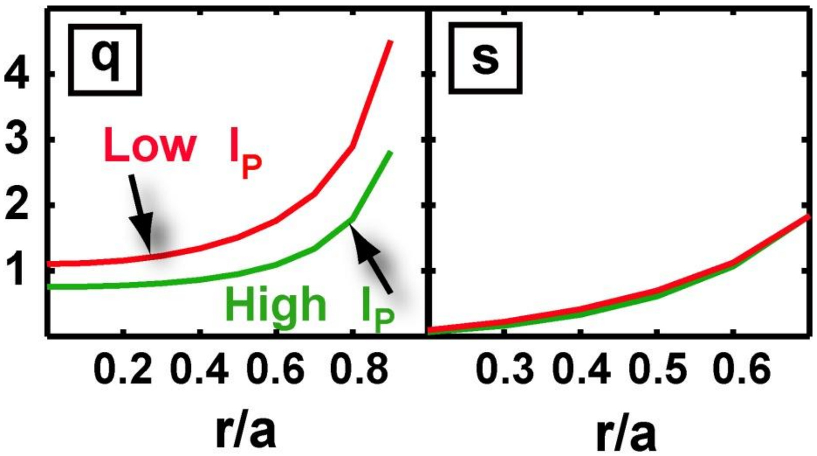

Ongoing Work

- **Impurity charge scan during the same discharge: He^{2+} (*injected*), C^{6+} (*intrinsic*)**
  - **Increasing Z indicates a weaker accumulation**
  - **Possible explanation is a decreasing inward thermodiffusion pinch ~ 1/Z**

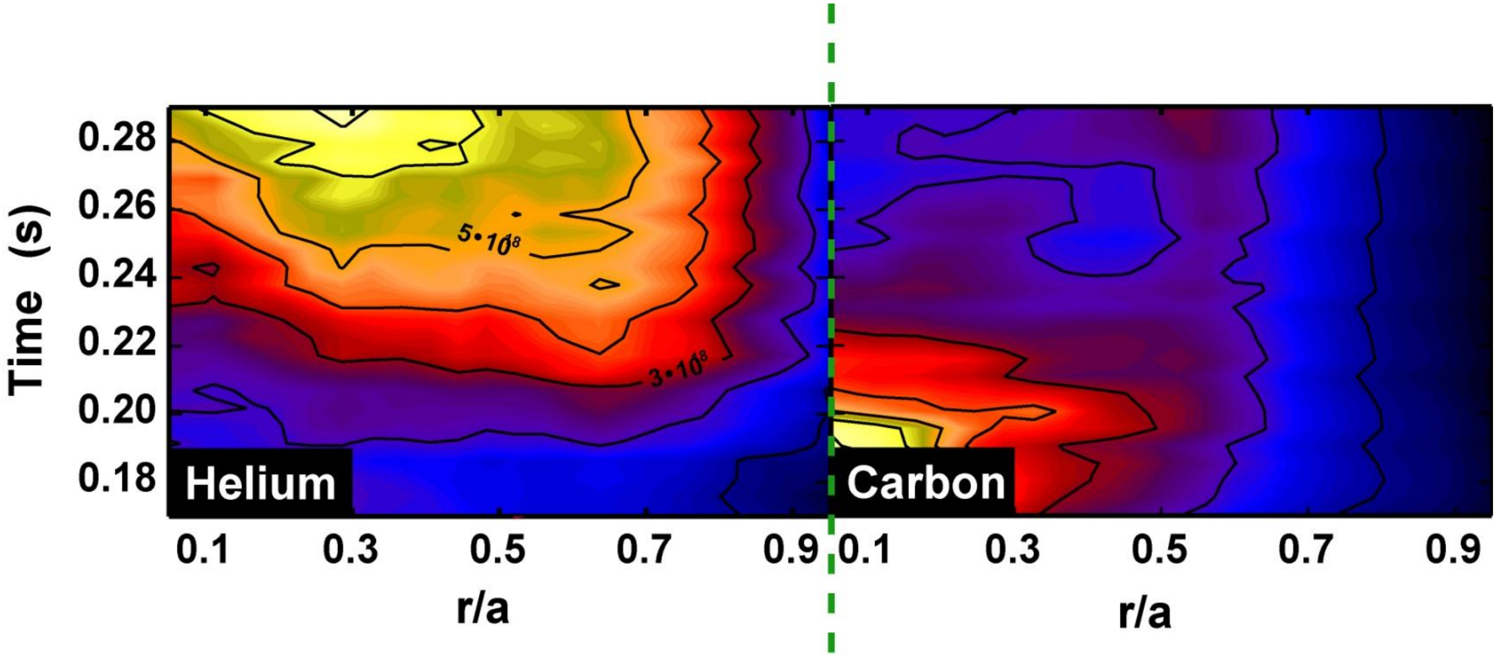

Ongoing Work

- Impurity charge scan during the same discharge: He^{2+} (*injected*), C^{6+} (*intrinsic*)
  - Increasing Z indicates a weaker accumulation
  - Possible explanation is a decreasing inward thermodiffusion pinch ~ 1/Z
- Next experimental campaign will look at Nitrogen (Z=7) transport
  - Expect further decrease inward thermodiffusion term?

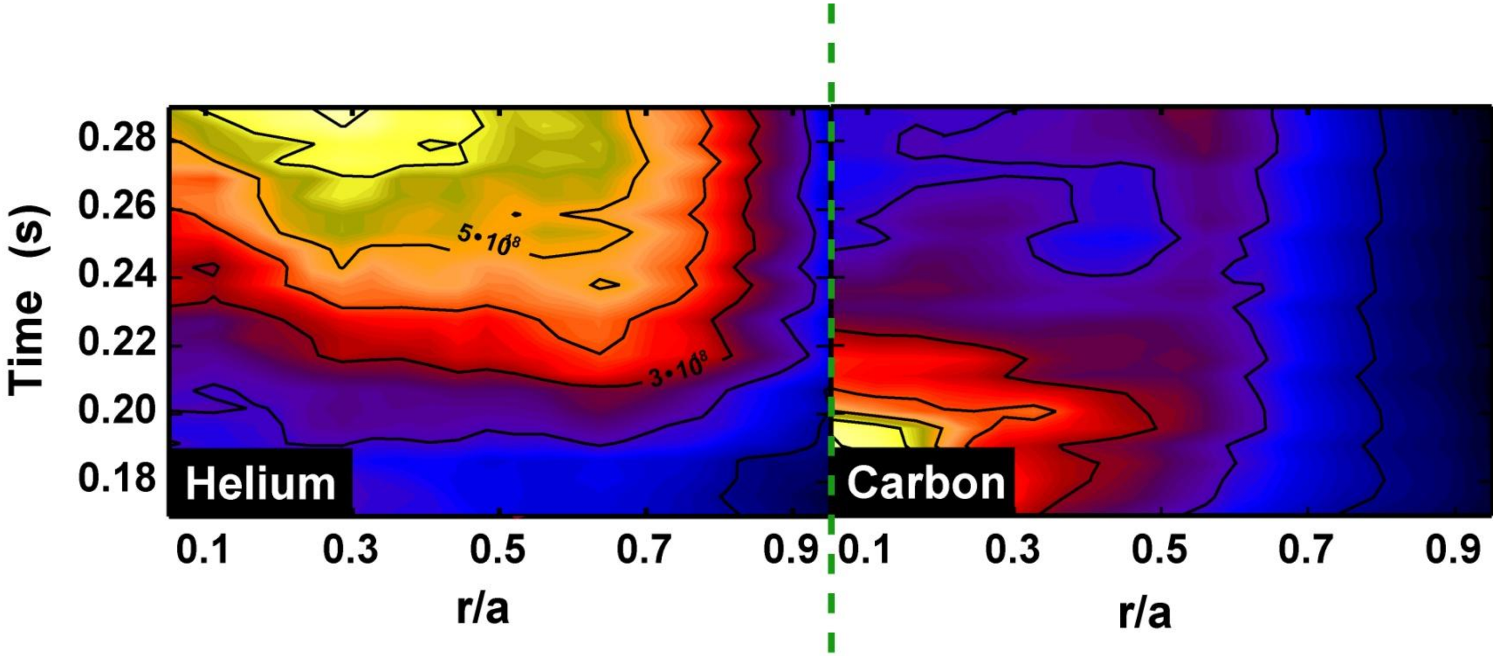

Conclusions

- **First experimental impurity transport analysis of carbon and helium on MAST**
  - **H-mode impurity transport close to neoclassical (r/a < 0.8)**
  - **L-mode impurity transport increasingly anomalous from core to edge**

Conclusions

- **First experimental impurity transport analysis of carbon and helium on MAST**
  - **H-mode impurity transport close to neoclassical (r/a < 0.8)**
  - **L-mode impurity transport increasingly anomalous from core to edge**
- **MAST H-mode indicates screening of impurities**
  - **Neoclassical effect**
  - **Positive or weak plasma ion density gradient**
  - **Agrees with current NSTX neon transport results**

Conclusions

- First experimental impurity transport analysis of carbon and helium on MAST
  - H-mode impurity transport close to neoclassical ($r/a < 0.8$)
  - L-mode impurity transport increasingly anomalous from core to edge
- MAST H-mode indicates screening of impurities
  - Neoclassical effect
  - Positive or weak plasma ion density gradient
  - Agrees with current NSTX neon transport results
- MAST L-mode shows strong and weak impurity accumulation during I_p scan at constant $B\phi$
  - Increasing I_p caused an outward trend in impurity particle pinch
  - Decreasing safety factor drives an outward convection due to parallel compression

Conclusions

- First experimental impurity transport analysis of carbon and helium on MAST
  - H-mode impurity transport close to neoclassical ($r/a < 0.8$)
  - L-mode impurity transport increasingly anomalous from core to edge
- MAST H-mode indicates screening of impurities
  - Neoclassical effect
  - Positive or weak plasma ion density gradient
  - Agrees with current NSTX neon transport results
- MAST L-mode shows strong and weak impurity accumulation during I_p scan at constant $B\phi$
  - Increasing I_p caused an outward trend in impurity particle pinch
  - Decreasing safety factor drives an outward convection due to parallel compression

Thanks for listening, any questions?

Appendix

Current Scan Conditions

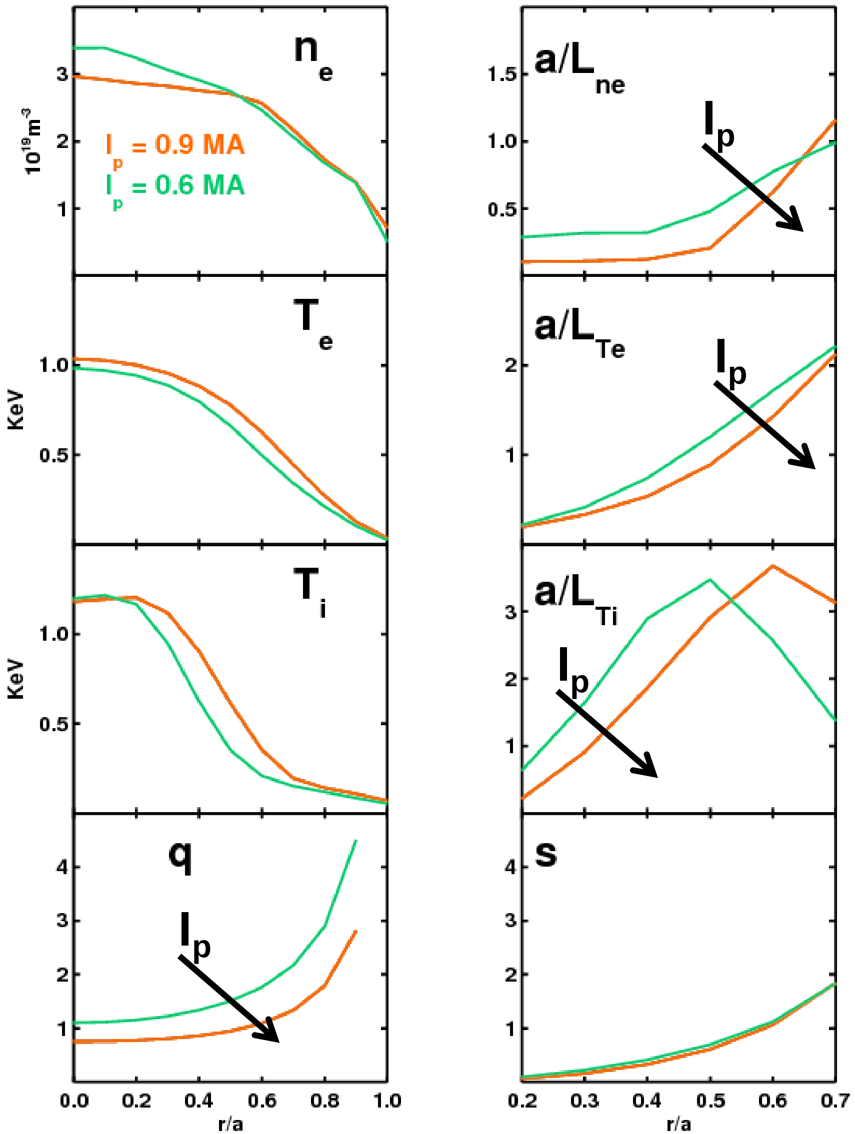

Carbon, L-mode Current Scan [A1]

• Increasing the current decreases the safety factor at constant B,

$$q_{eng} \propto \frac{B}{RI_p}$$

• Beam power has been kept constant during scan therefore T_e and T_i increase with I_p

• All drive/suppresion terms are observed to decrease with increasing plasma current

• Clear increase in q-profile is observed as current is decreased

[A1] Valovič M, Akers R, de Bock M, *etal*, Nucl. Fusion, **51**, 073045 (2011)

Current Scan Conditions

- High plasma rotation gives rise to Coriolis Compression Drift

Y Camenen, *etal*, Phys. Plasmas, **16**, 012503

- Rotation changes by less than a factor of 2

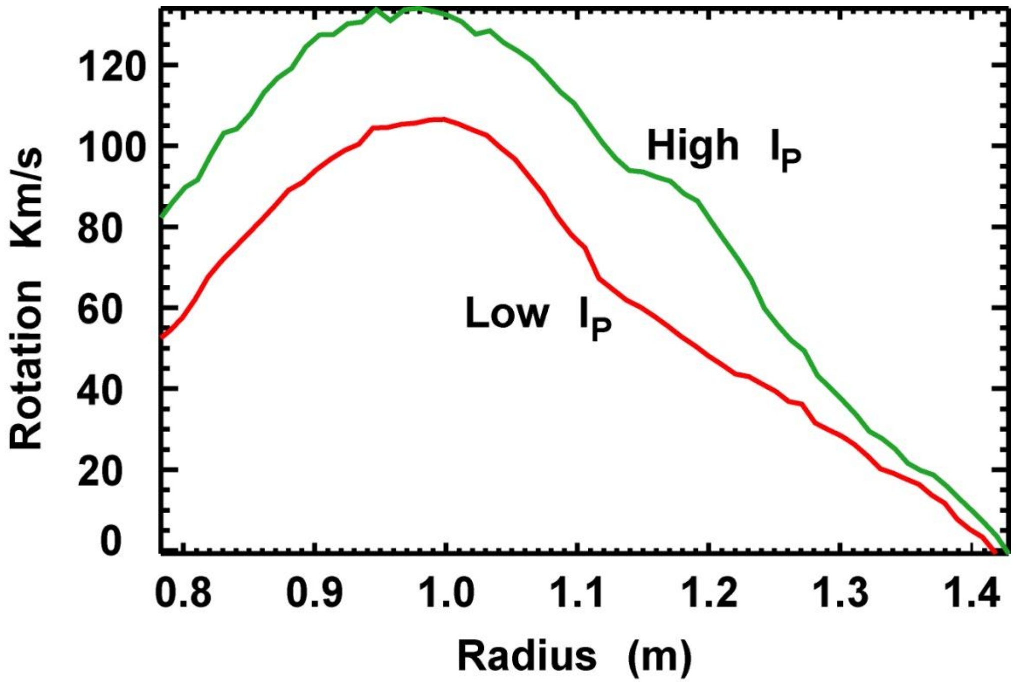

During the next experimental campaign on MAST, neutral beam power will be modified to compensate for ion temperature and rotation differences

Fluid Model Predictions

The set of fluid equations from the Weiland multi-fluid model are perturbed in impurity density, parallel velocity and temperature. From the impurity density response, the particle flux has been calculated to be [A2]:

$$\frac{\Gamma_{n_z}}{n_z c_s} = \frac{k_\theta \rho_s \tilde{\gamma} \left|\tilde{\phi}_k\right|^2}{|N|^2} \left[\frac{R}{2L_{n_z}}\left(|\tilde{\omega}|^2 + \frac{14\tau_z^*}{3}\tilde{\omega}_r + \frac{55\tau_z^{*2}}{9}\right) - \frac{R}{2L_{T_Z}}\left(2\tau_z^*\tilde{\omega}_r + \frac{10\tau_z^{*2}}{3}\right) - \langle\lambda\rangle\left(|\tilde{\omega}|^2 + \frac{10\tau_z^*}{3}\tilde{\omega}_r + \frac{35\tau_z^{*2}}{9}\right) + \frac{Z}{A_z q_*^2 |N_1|^2}\left(\tau_z^*\left(\frac{19}{3}\tilde{\omega}_r^2 - \frac{1}{3}\tilde{\gamma}^2 + \frac{100\tau_z^*}{9}\tilde{\omega}_r - 5\tau_z^{*2}\right) + 2\tilde{\omega}_r|\tilde{\omega}|^2\right)\right]$$

Diffusive flux

Curvature Pinch

Thermodiffusion Pinch

Parallel Compression Pinch

- **Diffusive flux** — ***~ R/L$_{NZ}$***
- **Thermodiffusion** — ***~ (1/Z)(R/L$_{TZ}$) inwards (ETG/TEM) or outwards (ITG)***
- **Curvature Pinch** — ***~ ∇q/q usually inwards***
- **Parallel impurity compression** — ***~ (Z/Aq^2) inwards (ITG) or outwards (ETG/TEM)***

[A2] H Nordman *etal* Plasma Phys. Cont. Fus., **53**, 105005 (2011)

Previous Alcator C-Mod Results

Argon gas puff experiment during an L-mode I_p-scan at constant B [A3]

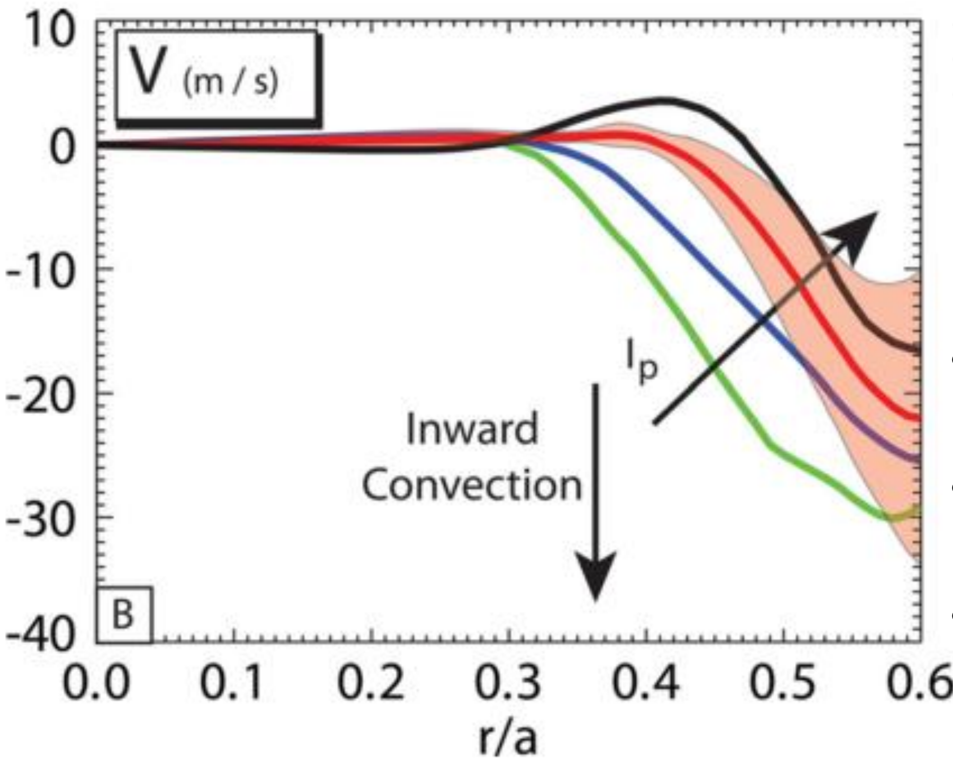

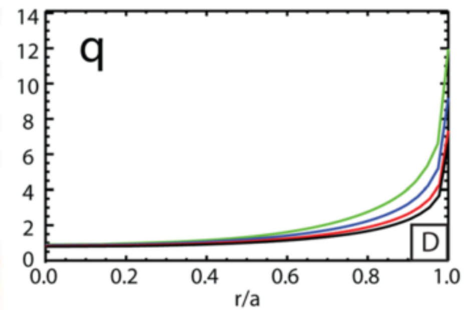

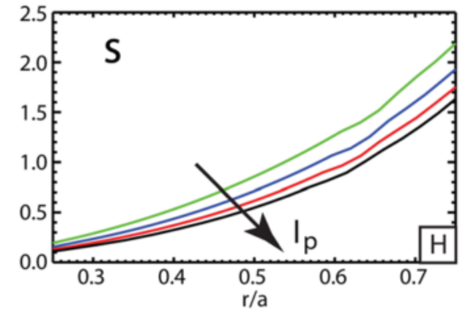

- **Small change in q**
- **Shear decreases with increasing I_p**
- **Reduces inward curvature pinch**

[A3] N Howard *etal*, Phys. Plasma, **19**, 056110 (2012)

Diagnostic Detail and Output

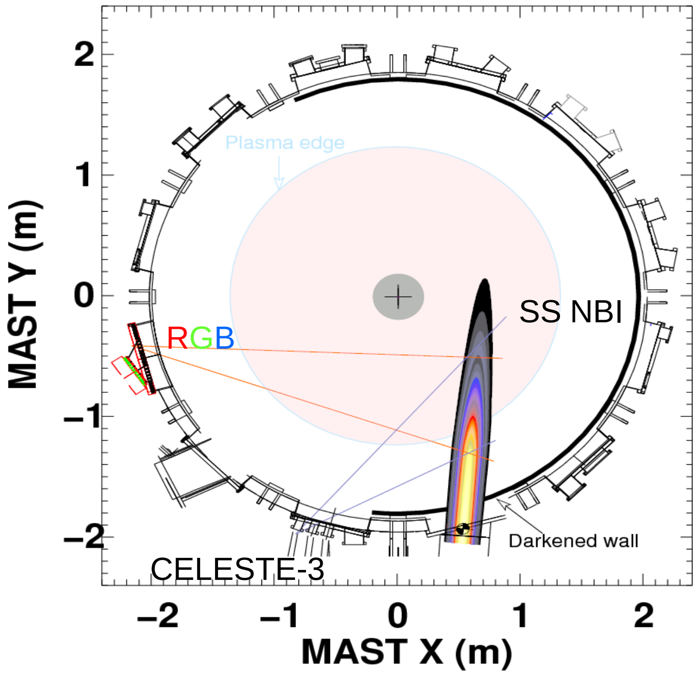

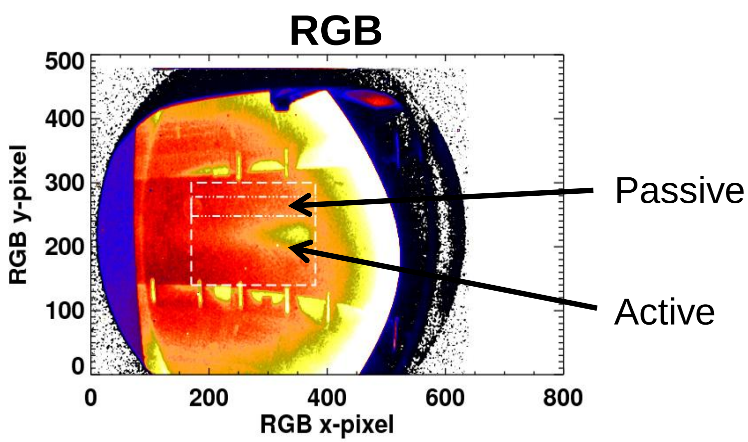

RGB – Carbon Channel (λ = 529.3 nm)

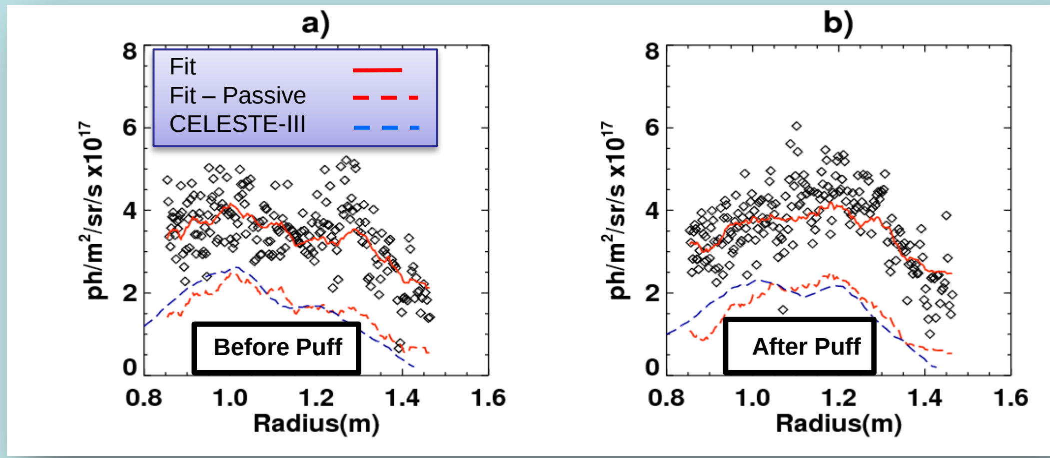

RGB – Helium Channel (λ = 468.8 nm)

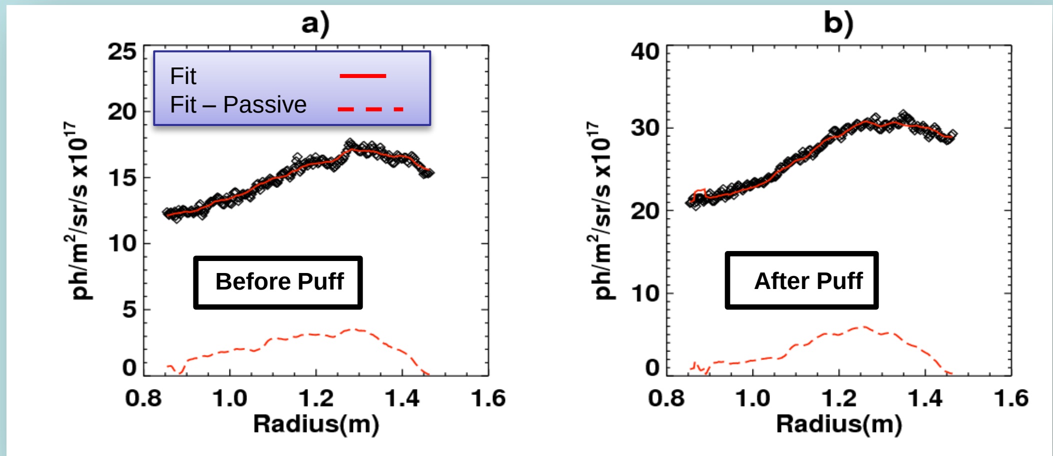

Carbon Raw Signal – Fit Method

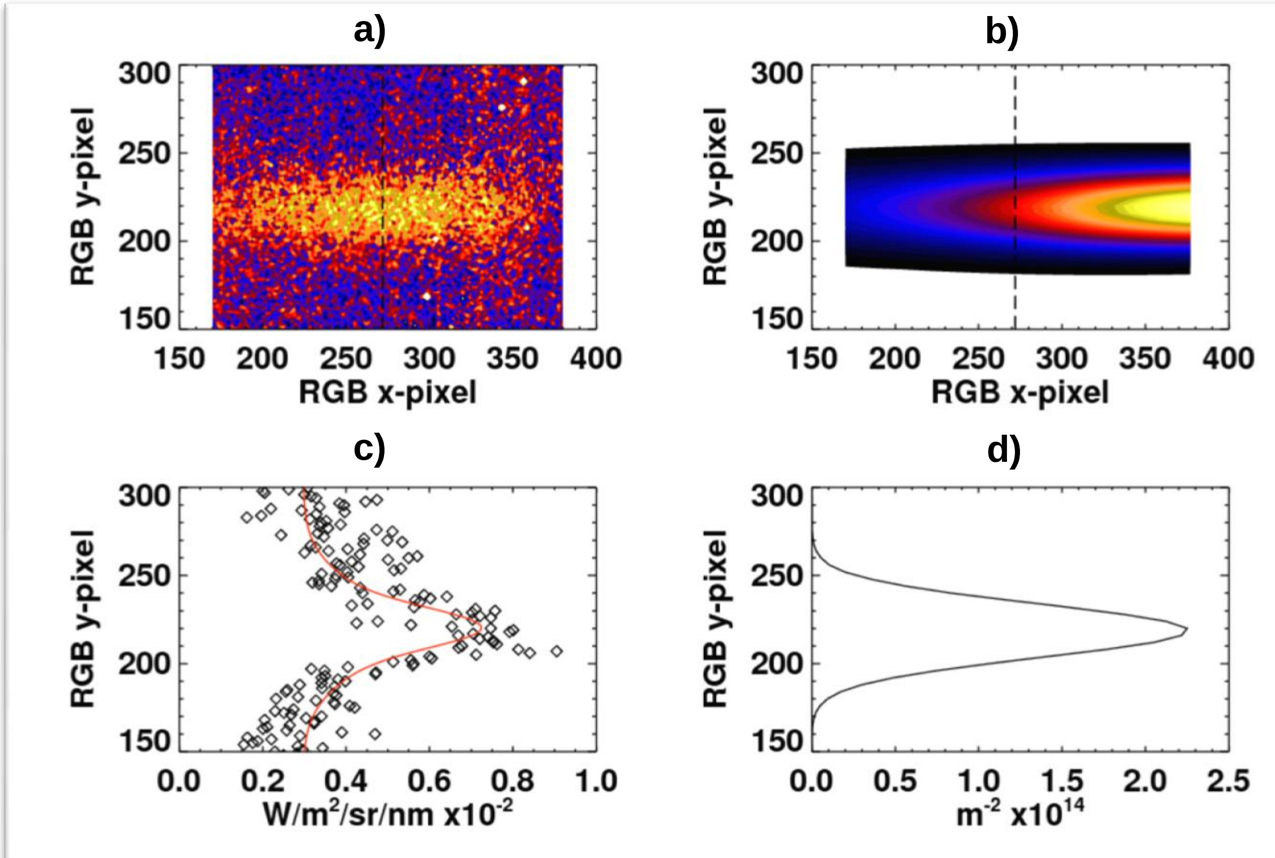

a) 2D image of raw RGB carbon channel

b) Forward model of neutral beam density (discussed later)

c) Vertical slice through raw RGB data

d) Vertical slice through neutral beam density

- Assumes CX emission scales with neutral beam density

Gradient Flux Approach

L-mode #28318
Sources/Sinks = 0 (Bad Assumption)